

# Vacuum Failsafe System and MOT Data Analysis for the ATTA Project

Christopher Stevens  
University of South Florida

XENON100 Experiment  
Atom Trap Trace Analysis Project

Advisors:  
Professor Elena Aprile and Professor Tanya Zelevinsky

August, 2011

## Abstract:

This paper presents the preliminary results of the Atom Trap Trace Analysis (ATTA) project' as well as the design and implementation of a vacuum failsafe system. Through the analysis of time delayed pictures, the Magneto Optical Trap's (MOT) loading rate, efficiency, and lifetime were determined. The expected results of the installation of a zero-length cube are also presented.

## Table of Contents

1. Introduction	
1.1 Dark Matter . . . . .	3
1.2 The XENON100 Experiment . . . . .	3
1.3 Xenon as a Detection Material . . . . .	3
2. ATTA Project	
2.1 Overview . . . . .	4
2.2 Laser Cooling . . . . .	4
2.3 Magneto Optical Trap . . . . .	5
3. Experiment	
3.1 Vacuum Failsafe System . . . . .	5
3.1.1 Interfacing the Two Devices . . . . .	6
3.1.2 Failsafe Circuit . . . . .	6
3.2 Zero-Length Cube . . . . .	7
3.3 MOT Image Analysis . . . . .	8
3.3.1 ROOT Code . . . . .	8
3.3.2 Analysis Process . . . . .	8
3.3.2a CCD Detection . . . . .	8
3.3.2b Photodiode Detection . . . . .	9
3.3.3 Analysis . . . . .	9
4.1 Results . . . . .	10
5.1 Conclusion . . . . .	10
5.2 Acknowledgements . . . . .	10
6. References . . . . .	12

# 1. Introduction

## 1.1 Dark Matter

Through numerous observations, strong evidence has been acquired for the existence of dark matter. Dark matter makes up roughly 23% of the energy density of the universe as determined by the Wilkinson Microwave Anisotropy Probe (WMAP) [1]. Today we know that 4.6% of the universe is made of the atoms and matter we see, baryonic matter, while the rest is made of non-baryonic matter [1].

The first evidence for dark matter came when Professor Fritz Zwicky studied the rotational speed of galaxies and their masses. From this, he determined that the galaxies were spinning too fast to be held together by the visible matter and postulated the existence of some sort of “dark matter” [2].

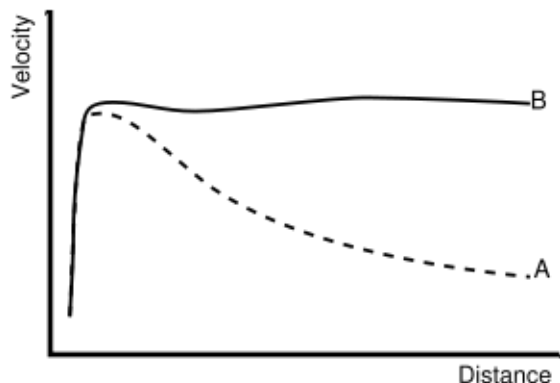


Figure 1: Curve A is the predicted rotational velocity of a galaxy as a function of distance from the center. Curve B is the measured values. [3]

Figure 1 shows the rotational velocity distribution of a typical galaxy. Curve A was the expected results with the given visible mass of the galaxy. Curve B was the actual measured data, which indicates the existence of large quantities of unseen mass holding the galaxy together.

Dark matter has not been directly detected yet. Its properties make this exceedingly difficult. The leading particle candidates for dark matter are those of the Weakly Interacting Massive Particle

(WIMP) class. These particles, as the name suggests, are weakly interacting (cross section of  $2 \times 10^{-45} \text{ cm}^2$ ) and are thought to have masses in the 10 to 1000 GeV range [4].

## 1.2 The XENON 100 Experiment

Since dark matter is so difficult to detect there are several criteria that the detector must meet. It must have an extremely low background ( $<0.0001$  events/kg/keV/day before rejections) [7], the nucleus of the detecting material must have many nucleons, the detecting material must be inert with no radioactive impurities, and the experiment must be able to decipher which events are from dark matter and which are not [5].

The XENON100 experiment meets these requirements. It uses a large vat containing  $\sim 170\text{kg}$  of liquid xenon (LXe) where 100kg is used for shielding purposes and 70kg as its detecting material [7]. Xenon is an inert noble gas with a large mass. It is also a scintillator, allowing visual detection methods to be possible. The detector is located in the Laboratori Nazionali Del Gran Sasso in Italy, which is beneath 3100m of rock. This rock helps prevent interactions from cosmic rays with the detector, thus lowering the background of the experiment. The muon flux is reduced by a factor of  $10^6$  due to this shielding [5].

## 1.3 Xenon as a Detection Material

Although Xe is an excellent detector material, attaining the ultra-high radio-purity necessary for a dark matter search is challenging. When xenon (Xe) is extracted from the atmosphere, it has several isotopes of krypton (Kr) present; some of which are radioactive. In commercially available Xe, Kr typically is present at the parts per million (ppm) level [6].  $^{85}\text{Kr}$  is a radioactive isotope that causes issues for dark matter detection. It beta decays with an end-point energy of 687 keV, and has a half life of 10.76 year. Although  $^{85}\text{Kr}$  is only  $\sim 10^{-11}$  of the Xe testing material [6],  $^{85}\text{Kr}$  nonetheless causes any dark matter results to be lost to background at the parts

per billion (ppb) level with the sensitivity of XENON100. This is seen in figure 2 which plots the sensitivity of the detector and the rate of events due to the decay of  $^{85}\text{Kr}$ , for the ppb and ppt levels. Therefore, this isotope must be removed to the parts per trillion (ppt) level in order to reach the sensitivity goal of the next phase of XENON detectors, XENON1T.

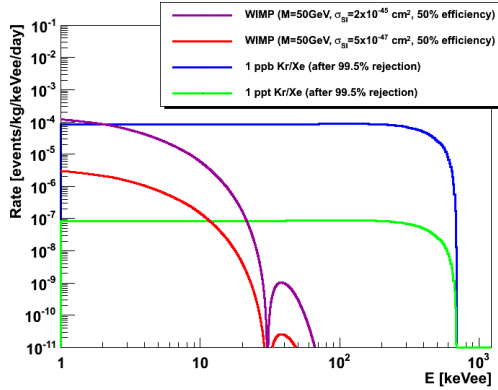


Figure 2: Detection rate of Kr/Xe at different purifications and sensitivity of the Xenon detector.

To remove the krypton isotopes from the xenon, the xenon gas is first purified by an outside company, Spectra Gases Company. This reduces the krypton's presence to 5-ppb [5]. To purify the xenon further, a cryogenic distillation column is used [6]. This method should reduce the krypton levels to the targeted ppt level. After purification, the abundance of  $^{85}\text{Kr}$  must be determined, and several experiments are underway to do this. One such experiment is the Atom Trap Trace Analysis (ATTA) project.

## 2. ATTA

### 2.1 Overview

Through the use of laser trapping techniques and single atom detection, the impurities in liquid xenon (LXe) can be determined. The Xe sample, in gaseous form, is pumped into the system, excited to the necessary metastable state, slowed, and trapped. Then, an image of the trapped atoms is taken and analyzed to determine the levels of  $^{84}\text{Kr}$  present in the sample. From this value, the amount of  $^{85}\text{Kr}$  can be

extrapolated using their previously measured relative isotopic abundance [7]. Figure 3 shows a schematic diagram of the experiment.

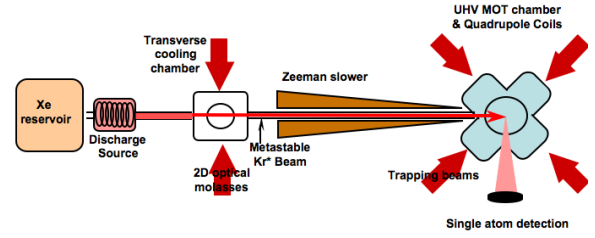


Figure 3: A schematic diagram of the ATTA experiment. [7]

### 2.2 Laser Cooling

The Xe atoms are cooled from the radiation pressure force. Since photons have momentum, when an object absorbs photons there is a change in its momentum [8]. This is from conservation of momentum. When a laser is shined on an atom and it absorbs the light, its momentum changes according to the radiation force:

$$F_{rad} = \frac{IA}{c} \quad (1)$$

where  $I$  is the light intensity,  $A$  is the area absorbing the light, and  $c$  is the speed of light [8].

For atoms moving opposite the laser propagation direction, the equation becomes:

$$F = \frac{-\sigma_{abs} I}{c} \quad (2)$$

where  $\sigma_{abs}$  is the cross-sectional area of the atom [8]. The laser light must be red detuned to compensate for the Doppler shift caused by the relative velocity of the atoms and the laser source. The laser detuning is calculated from:

$$\omega' = \omega + kv \quad (3)$$

where  $\omega'$  is the laser frequency,  $\omega$  is absorption frequency of an atom at rest,  $k$  is the wave number, and  $v$  is the atoms velocity [8]. This ensures the laser is the correct frequency for the atoms to absorb the laser light. Each time an atom absorbs a photon it reemits the photon in a random

direction, resulting in a momentum kick. This process gives the atoms a net force against its direction of motion, causing the atom to slow.

However, as the atoms slow, the laser frequency is no longer on resonance and will no longer interact with the atoms. To compensate for this, a Zeeman slower is used. A Zeeman slower is a spatially varying magnetic field. ATTA uses a solenoid that varies in its number of wrappings along its axis. The magnetic field changes the hyperfine energy levels of the atoms, and therefore their resonance frequency. This is done in such a way that as the atoms slow the laser will always be on resonance for the peak velocity distribution [8].

ATTA also uses a two dimensional optical molasses, which consists of pairs of counter-propagating, red-detuned laser beams. The optical molasses is used to collimate atoms in the direction of the trap by removing their transverse velocities. Effective collimation is achieved by bouncing the laser beams back and forth against mirrors slightly off parallel, so as to affect the atoms for a longer period of time.

## 2.3 Magneto Optical Trap

After the atoms are slowed and exit the Zeeman slower, they enter the Magneto Optical Trap (MOT). The MOT uses a three dimensional optical molasses and a pair of anti-Helmholtz coils as seen in figure 4 (parallel current loops, with the current running in opposite directions).

The MOT traps the atoms using the radiation force and a spatially varying magnetic field. The magnetic field at the center of the trap is zero and increases linearly as you move outward in any direction [8]. When the atoms enter the MOT, they will encounter the magnetic field. This field changes the atoms resonance frequency to match that of one of the lasers so the atom is pushed to the center. The imbalance in the radiation pressure force is due to the atom still having velocity. The velocity causes a Doppler shift so that the laser is closer to resonance in one direction compared to the other. Since it

is closer in one direction, the force is greater and pushes the atom to the center. This force obeys the following equation:

$$F_{MOT} = -\alpha v - \frac{\alpha\beta}{k}z, \alpha = 2k \frac{\partial F}{\partial \omega} \quad (4)$$

where  $\alpha$  is the damping coefficient,  $v$  is the velocity,  $\beta$  is the Zeeman shift,  $k$  is the wave number, and  $z$  is the atoms displacement from the center of the MOT. This effect takes place in all three spatial degrees of freedom.

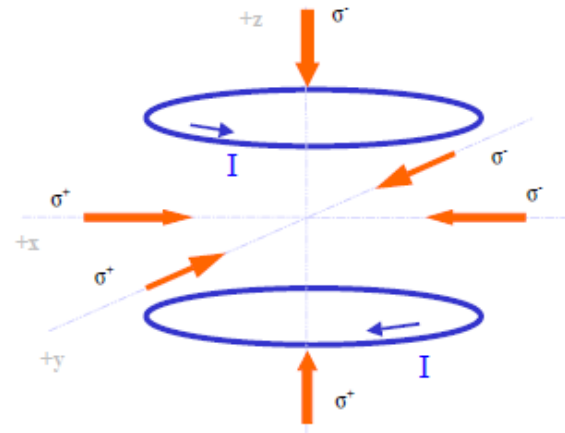


Figure 4: Schematic of three-dimensional trapping using a MOT.

The radiation force only balances out at the center of the MOT. At this point, the magnetic field is zero. When the atoms try to leave this area, they encounter the radiation force and are pushed back to the center. When they are in the center with zero velocity, the radiation force cancels in all directions since there is no Doppler shift. Thus, the atom is trapped [8].

## 3. Experiment

### 3.1 Vacuum Failsafe System

The purpose of the experiment was to develop a failsafe circuit for the vacuum system, so that in the event of power failure or equipment malfunction, the vacuum is maintained within the system and the damage to the pumps is minimal. This

was composed of three valves, the main vacuum pump, and a circuit to connect the two.

### 3.1.1 Interfacing the Two Devices

For the failsafe to work, the vacuum pump and the valves needed to be able to talk to each other. Should the vacuum ever encounter an error and shutdown, the valves need to immediately shut.

The valves (VAT Series 012, DN 16-50, with solenoid) are powered by compressed air and electricity. The electricity holds the valve open and should the valve lose power, the compressed air forces it closed.

The vacuum pump (Pfeiffer HiCube 80 Eco) uses a drive unit (Pfeiffer TC 110) for power. This drive unit has error reporting capabilities in the form of a voltage output. When the vacuum is running without errors, pin 9 on the drive unit outputs 24V. If the vacuum encounters an error or loses power, this voltage drops to zero.

Using these two characteristics of the devices, a simple circuit can be constructed to allow these devices to interact.

### 3.1.2 Failsafe Circuit

The circuit used to connect these two devices is shown in figure 5. The parts needed for the circuit are one normally open 24V voltage relay (Crydom CX-E-240-D-5-R), three Single Pull Double Throw (SPDT) switches (SP1 100 series), three female NEMA-15 power connectors, one green LED, one 27kΩ resistor, and one 600Ω resistor.

Since the voltage relay is normally open, the 24V that the vacuum puts out when functioning correctly closes it. This allows the AC current to flow through the relay to the manual switches and the female NEMA-15 VAC power connectors. The valve power cords can be plugged directly into the box supplying them with power.

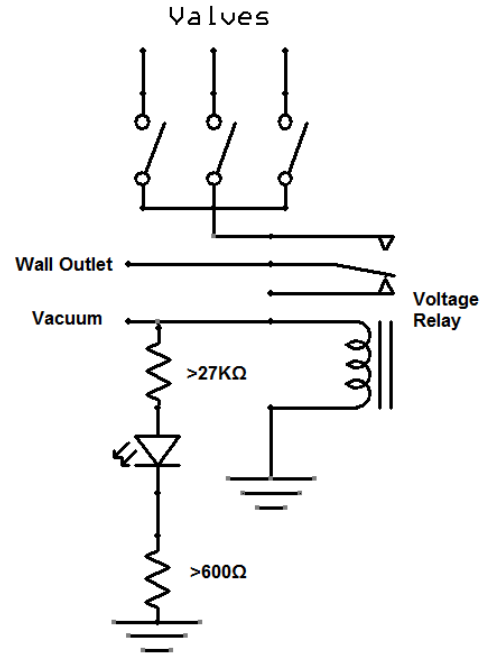


Figure 5: Diagram of the circuit used to maintain the vacuum in case of a pump malfunction or power failure.

The voltage from the vacuum is used to power an LED as well. This LED is used as a signal that the vacuum is working correctly. The 600Ω resistor following the LED is there to protect it and to lower the 24V. The value of this resistor was determined from the following equation:

$$R = \frac{V_s - V_l}{I} \quad (5)$$

where R is the resistance needed,  $V_s$  is the supply voltage,  $V_l$  is the maximum voltage for the LED, and I is the maximum current for the LED. This equation can be obtained from ohms law. The 27kΩ resistor was installed after the circuit was complete to tone down the brightness of the LED.

Finally, there are manual switches to cut the power to the individual valves in case a single valve needs to be closed (i.e. to work on the system but maintain the vacuum in other parts).

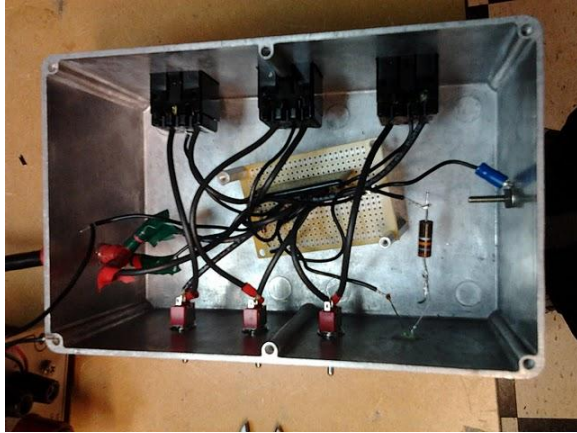


Figure 6: The picture above is the finished circuit as seen from above the box.

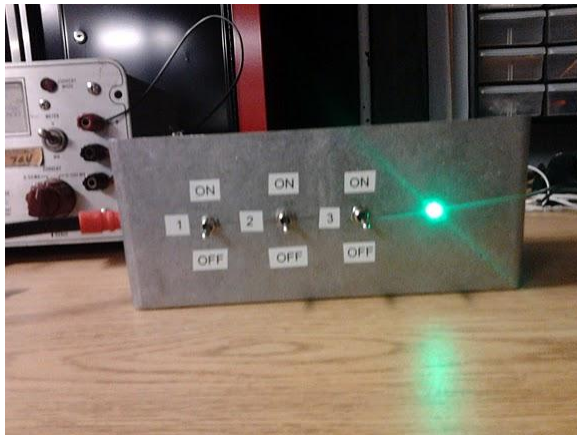


Figure 7: This is the front of the circuit box which shows the manual switches for the valves as well as the operational LED.

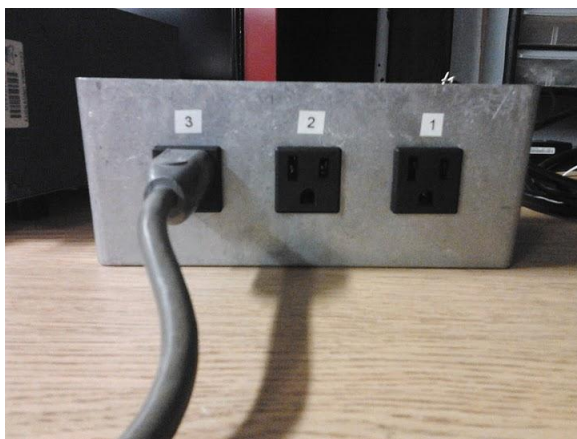


Figure 8: This is the back of the box for where the valve power cords will be plugged.

### 3.2 Zero-Length Cube

To increase the efficiency of the system, a section of the ultra-high vacuum pipe was switched out. A six-way cross (figure 9) was replaced with a zero-length cube (figure 10). This part is located near the source before the Zeeman slower.



Figure 9: High vacuum tubing when six-way cross was installed with the source removed.

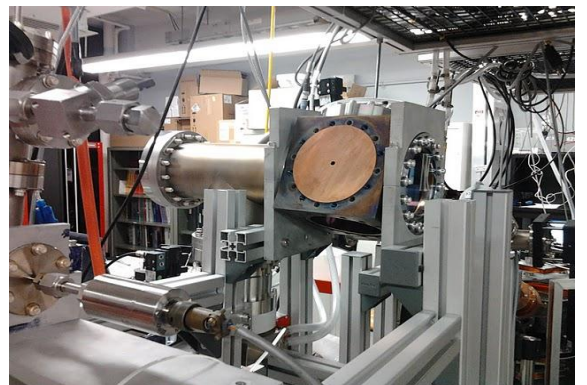


Figure 10: High vacuum tubing after the zero-length cubed was installed with the source removed.

When the atoms entered the six-way cross, they had to travel  $\sim 10\text{cm}$  before encountering the transverse cooling (two dimensional optical molasses). During those  $10\text{cm}$ , the atoms had time to disperse. This causes the cloud density to greatly decrease by roughly a factor of  $1/d^2$ . This also causes them to miss the transverse cooling and be lost to the system. This effect happens twice; once when the atoms first enter the system, and again when they leave the first transverse cooling.

By replacing the cross with a zero-length cube, these two areas are eliminated. This is expected to increase the efficiency of the system by a factor of ~10-15.

### 3.3 MOT Image Analysis

The form of data that the ATTA experiment currently collects is images of the trapped atoms in the MOT. These images are taken by a HDCCD camera (Thorlabs DCU224M). A photodiode (Thorlabs DET36A) can also be used. From the analysis, several results were obtained; the MOT lifetime, the loading rate,  $\beta$ , which is a constant of atom collisions, and the dark background.

#### 3.3.1 ROOT Code

The data that is collected comes in the form of images. These images need to be processed into meaningful results. To do this, they are run through a ROOT program. This program first scans a given directory for the images. Then, it loads the images one at a time to be analyzed.

The analysis process takes the image and converts it to the individual pixel brightness. The brightness is also summed to determine the total image brightness. A two dimensional histogram is then filled with the data and the pixel brightness as the weights. The histogram is fit with a two dimensional Gaussian and the results are recorded. These fit results will be used later to determine the temperature in the trap. The total image brightness is also processed to determine the number of total atoms in the trap. This process is explained in the following section.

#### 3.3.2 Analysis Process

The number of atoms trapped in the MOT can be calculated from the number of photons detected by the CCD camera and extrapolating this over the entire sphere using the solid angle.

The first quantity that must be calculated is the scattering rate per atom, assuming the on-resonance saturation parameter,  $s_0$ , is much

greater than one. This assumption can be made due to the high laser intensities which saturates the atomic transition [9]. The scattering rate per atom is given by the following equation [9]:

$$\Gamma_s = \frac{s_0}{1+s_0} * \frac{\Gamma}{\left(1 + \left(\frac{2*\delta}{\Gamma}\right)^2\right)} \quad (6)$$

where  $\Gamma$  is the natural linewidth, or the decay width, of the atoms and  $\delta$  is the detuning of the laser due to the Doppler shift. This equation holds true for steady state situations.

$\Gamma$  is a property of the atom's metastable state; which the atoms have been excited to when they first entered the system. For argon, the current gas being tested with, the value of  $\Gamma$  is  $3.688 \times 10^7$  Hz.  $\delta$  is determined by the Doppler shift as discussed in section 2.2 and 2.3.

$S_0$  is equal to the laser intensity divided by the saturation intensity of the atom. Since there are three lasers reflected back on each other, the intensity,  $I$ , is calculated by:

$$I = 2(I_x + I_y + I_z) \quad (7)$$

and the saturation intensity of argon is a known property with a value of  $1.44\text{mW/cm}^2$ . This gives the photon scattering rate. A typical value for the scattering rate is on the order of  $10^6 - 10^9$  [Hz].

#### 3.3.2a CCD Detection

When the CCD camera is used to image the MOT, the number of atoms can be calculated from the image's total brightness. First, the solid angle is calculated. The CCD camera has a detection area of  $1.69\text{cm}^2$ . The camera is placed  $24.448\text{cm}$  away from the center of the MOT. The total surface area of a sphere with a radius of  $24.448\text{cm}$  is  $7510.98\text{cm}^2$ . This gives a fractional solid angle,  $\Omega_1$ , value of  $2.25 \times 10^{-4}$ .

The total number of photons detected by the CCD camera a second is also necessary. To calculate this, the following equation is used:



$$\varphi d_1 = \frac{(511)B_{tot}}{T_{exp}} \quad (8)$$

where  $B_{tot}$  is the total brightness of the image and  $T_{exp}$  is the exposure time of the camera. The 511 comes from a property of the CCD camera that was measured. This was done by exposing the CCD camera to a very weak beam, such that the camera does not become saturated. An image was taken with a given exposure time and laser power. From the power and exposure time, the energy can be calculated:

$$E = P * T_{exp} \quad (9)$$

and divided by the energy of an individual photon with a wavelength of 811.75nm. This gave  $2.4 \times 10^9$  photons. This was then divided by the total brightness of the image which gave 511 photons/brightness units for each pixel.

The total number of atoms in the MOT is determined by equation 10. The number of photons detected per second is divided by the photon scattering rate as well as the geometric fraction.

$$\# \text{ of atoms} = \frac{\varphi d_1}{\Gamma_s \Omega_1} \quad (10)$$

### 3.3.2b Photodiode Detection

If the photodiode is used to view the trap, then a different analysis is needed. First, the photodiode's solid angle is calculated. It has a detecting area of  $0.13\text{cm}^2$  and the total surface area of the sphere is the same as with the CCD camera. Dividing these two values yields a fractional solid angle,  $\Omega_2$ , value of  $1.73 \times 10^{-5}$ .

Next, the number of photons detected by the photodiode a second,  $\varphi d_2$ , is calculated. This value is calculated by the following equation using the characteristics of the photodiode and the energy of the photons:

$$\varphi d_2 = \frac{V}{(Res)(R)} \frac{\lambda}{hc} \quad (11)$$

where  $V$  is the voltage output,  $R$  is the scope coupling impedance, and  $Res$  is the responsivity in  $A/W$  of the photodiode.  $\lambda$  is the wavelength of the emitted photon and has a value of 811.75nm,  $h$  is planck's constant, and  $c$  is the speed of light.

Finally, the number of atoms can be obtained by taking into account the total number of photons detected per second, the scattering rate of these photons, and the solid angle. This is done by combining equations (6), (8) and the solid angle:

$$\# \text{ of atoms} = \frac{\varphi d_2}{\Gamma_s \Omega_2} \quad (12)$$

This provides the total number of atoms present in the trap.

### 3.3.3 Analysis

The meaningful results that can be extracted from the number of trapped atoms are the dark background level, the MOT loading rate, the MOT lifetime,  $\tau$ , and a characteristic constant,  $\beta$ . These results are found through numerical analysis of the number of photons detected as a function of time and the number of atoms trapped as a function of time.

Three graphs were made. The first one plots  $p$  the number of photons detected as a function of time starting with no atoms trapped. The second one started with no atoms trapped, and took pictures in a specified time interval to see how the trap forms. The third starts out with a stable trap, and takes consecutive pictures to watch the trap decay with time, once the loading of atoms into the trapped is stopped. From the first graph, the dark background is determined. The second graphs allow for the trap loading rate to be determined. The MOT lifetime and  $\beta$  are obtained from the third graph.

The equation that models the trap has been proven to be the following [10]:

$$\frac{dN}{dt} = L - \frac{N}{\tau} - \beta N^2 \quad (13)$$

where  $dN/dt$  is the change in the number of trapped atoms,  $L$  is the loading rate,  $N$  is the number of trapped atoms,  $\tau$  is the trap lifetime, and  $\beta$  is a characteristic of the trapped atoms colliding with themselves. The first term,  $N/\tau$ , is from the collisions between the trapped atoms and the thermal background atoms [10]. The second term,  $\beta N^2$ , is from the trapped atoms colliding with each other. For a high loading rate, the second term becomes dominant allowing the first term to be ignored.

However, when the trap is first being loaded, the second term can be ignored since there are not enough trapped atoms to have a significant amount of collisions. Also, there are no atoms initially trapped in the MOT. Therefore, the loading rate is an exponential function (linear at short times) that passes through the origin when the dark background is removed.

Graphing the number of photons detected versus time while the trap is loaded and fitting the first few points with a linear fit allows for the dark background to be determined. The dark background becomes the y intercept of the fit.

Graphing the number of atoms versus time while the trap is being loaded, you can then determine the loading rate by fitting the first few points to a linear fit. After some time, the trap will begin to reach equilibrium making the graph no longer linear. This is because the second term can no longer be ignored due to the collisions between two trapped atoms. From the linear fit, the slope is the MOT loading rate.

By solving equation (13) while saying the loading rate is zero, one can obtain an equation that models the decay of the trap. This solution is:

$$N(t) = \frac{1}{\left(\tau\beta + \frac{1}{N_0}\right)e^{t/\tau} - \tau\beta} \quad (14)$$

where  $N_0$  is the initial number of atoms in the trap. By fitting the trap decay plot with this equation,  $N_0$ ,  $\beta$ , and  $\tau$  can be determined.

## 4.1 Results

Figures 11, 12, and 13 show the data obtained before the six-way cross was replaced for the zero-length cube.

Figure 11 shows the number of photons detected as a function of time while the trap is being loaded. The trap was initially empty. Fitting the first ~5 points with a linear fit gave the following results. The dark background level is  $1.523 \pm .092 \times 10^6$  [photons]

Figure 12 shows the number of atoms in the trap as a function of time after the dark background was removed. This gives a loading rate of  $3.78 \pm 0.17 \times 10^4$  atoms/s.

The system's consumption rate is  $9.2 \times 10^{16}$  atoms/s. This consumption rate was experimentally determined prior to these measurements. Using this consumption rate gives a system efficiency of  $4.11 \pm 0.18 \times 10^{-13}$ .

Figure 13 shows a graph of how the MOT decays as a function of time. It shows the MOT lifetime to be  $1.529 \pm 0.047$  [s]. The values of  $N_0$  and  $\beta$  are  $97340 \pm 852$  [atoms] and  $5.15 \pm 0.49 \times 10^{-6}$  [1/atoms\*s], respectively. These results are summarized in figure 14.

## 5.1 Conclusion

When the experiment is optimized with the zero-length cube, the expectations for the experiment are as follows. The expected value for the loading rate is  $4.5 \pm 0.79 \times 10^5$  [atoms/s], which gives an efficiency of  $4.93 \pm 0.82 \times 10^{-12}$ . This is based on a factor of 12 increase in efficiency. This changed the number of trapped atoms at equilibrium. The value,  $N_0$ , is expected to be  $1.16 \pm 0.19 \times 10^6$  [atoms].

These values are expected to be improved further by adding a source cooling system. Assuming a Maxwell-Boltzmann distribution, this will increase the number of atoms slowed in the system from 6% to 29%.

## 5.2 Acknowledgements

I would like to personally thank Luke Goetzke and Tae-Hyun Yoon for all of the help this summer and the knowledge they passed onto me. I would also like to thank Elena Aprile and Tanya Zelevinsky for overseeing and managing this experiment as well as the XENON100 collabora-

tion. Also, the National Science Foundation for financing the summer research for undergraduate's program and Columbia University, in particular John Parsons, for running it and allowing me this research opportunity.

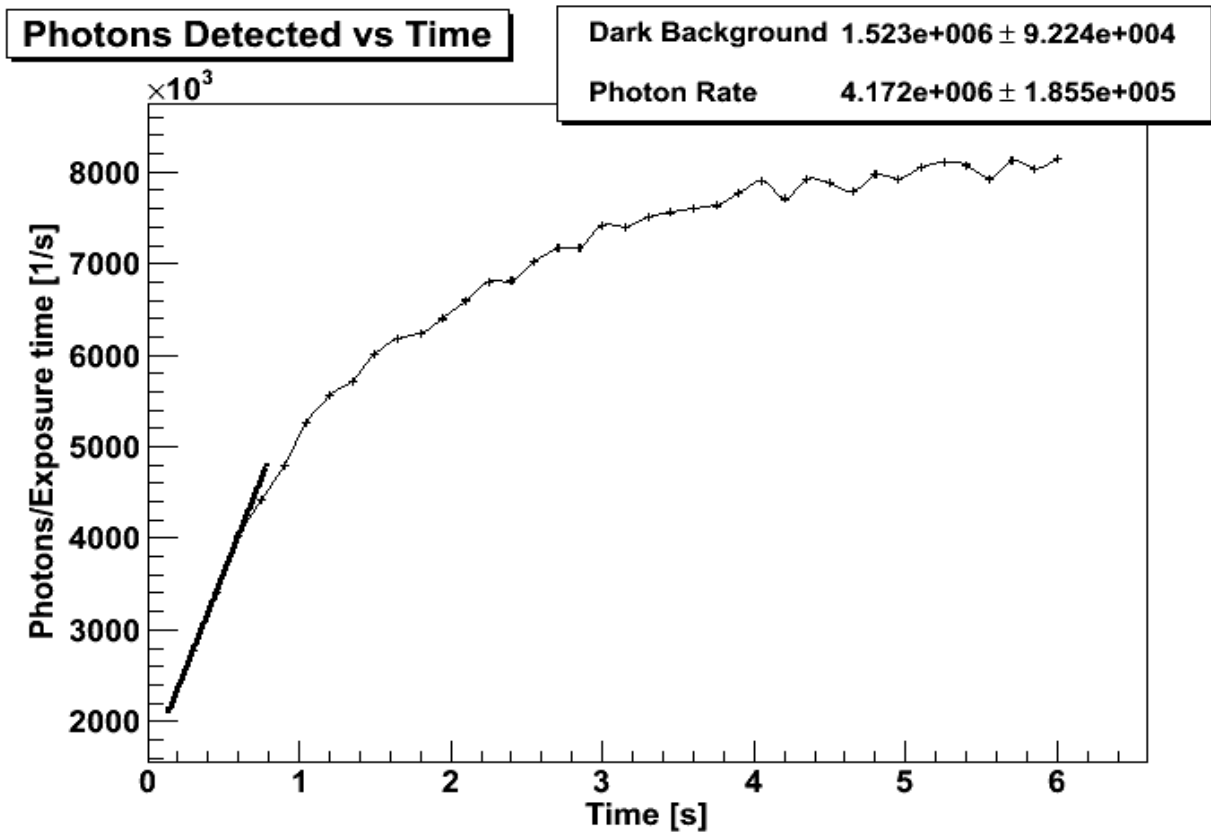


Figure 11: The above graph shows the number of photons detected as a function of time starting with the dark background. The background is  $1.523 \pm 0.092 \times 10^6$  photons. The error in the individual points is the square root of the number of photons.

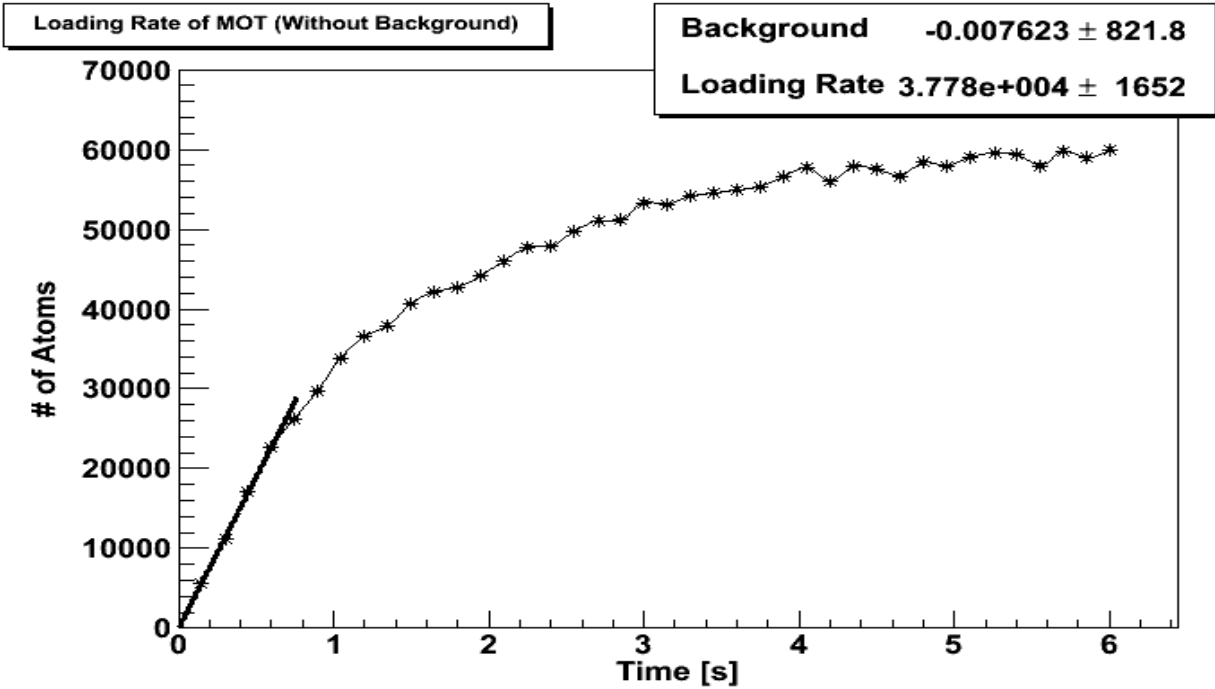


Figure 12: The above graph shows the number of trapped atoms as a function of time starting with no atoms trapped. This is after the dark background has been removed. The background value is  $0.00 \pm 820$  atoms, which is negligible. The Loading rate is  $3.78 \pm 0.17 \times 10^4$  atoms/s. The error in the individual points is the square root of the number of atoms.

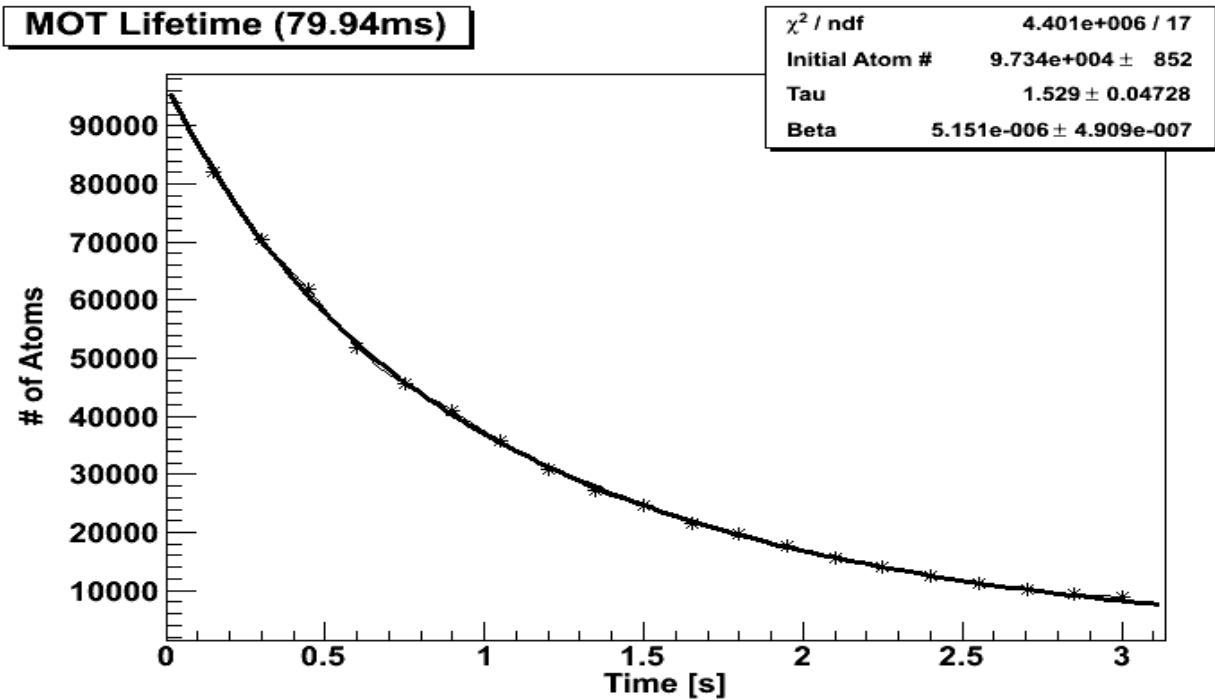


Figure 13: The above graph shows the decay of the MOT as a function of time. This was fit to the theoretical equation. This equation gives a MOT lifetime of 1.03 [s]. The error in the individual points is the square root of the number of atoms.

	Before Cube was installed	After Cube was installed - Expected
Dark Background [# of Photons]	$1.523 \pm 0.092 \times 10^6$	$1.523 \pm 0.092 \times 10^6$
Loading Rate [atoms/s]	$3.78 \pm 0.17 \times 10^4$	$4.5 \pm 0.79 \times 10^5$
System Efficiency	$4.11 \pm 0.18 \times 10^{-13}$	$4.93 \pm 0.82 \times 10^{-12}$
Initial # of Atoms [s]	$97340 \pm 852$	$1.16 \pm 0.19 \times 10^6$
Tau [s] – MOT Lifetime	$1.529 \pm 0.047$	$1.529 \pm 0.047$
Beta [1/Atoms *s]	$5.15 \pm 0.49 \times 10^{-6}$	$5.15 \pm 0.49 \times 10^{-6}$

Figure 14: The above table summarizes the results from the experiment before and after the six-way cross was replaced with the zero-length cube.

## 6. References

1. *Universe 101: Our Universe*. <[http://map.gsfc.nasa.gov/universe/uni\\_matter.html/](http://map.gsfc.nasa.gov/universe/uni_matter.html/)>.
2. Sidney Van Den Bergh. 19 April 1999. "The Early History of Dark Matter". PASP June 1999 issue. <[http://arxiv.org/PS\\_cache/astro-ph/pdf/9904/9904251v1.pdf](http://arxiv.org/PS_cache/astro-ph/pdf/9904/9904251v1.pdf)>
3. *How can we measure the mass of a galaxy?* <<http://www.astro.cornell.edu/share/sharvari/websiteV7/darkmatter.htm>>.
4. *Direct Detection WIMP Dark Matter*. <<http://cdms.berkeley.edu/Education/DMpages/science/directDetection.shtml>>.
5. *The XENON Detector*. <<http://xenon.physics.rice.edu/detector.html>>.
6. The XENON Dark Matter Project. <[http://xenon.astro.columbia.edu/XENON100\\_Experiment/](http://xenon.astro.columbia.edu/XENON100_Experiment/)>.
7. E. Aprile, T. Zelevinsky. *Instrument Development for Liquid Xenon Dark Matter Searches. An Atom Analysis System to Measure Ultra-Low Krypton Contamination in Xenon*. Columbia University, January 20, 2009.
8. Foot, Christopher. *Atomic Physics*. Oxford University Press. Pg 140 – 150. 2005.
9. Metcalf, Harold. *Laser Cooling and Trapping*. Springer-Verlag New York. Pg 10-16. 1999.
10. Du, Xu. *Realization of Radio-Krypton Dating With an Atom Trap*. Northwestern University. June 2003.